QUASI-ELASTIC LIGHT SCATTERING FROM MIGRATING CHEMOTACTIC BANDS OF *ESCHERICHIA COLI*.

III. Studies of Band Formation Propagation and Motility in Oxygen and Serine Substrates

PAUL C. WANG* AND SOW-HSIN CHEN‡

**Department of Radiology, Georgetown University, Washington, D.C. 20007; and ‡Nuclear Engineering Department, Massachusetts Institute of Technology, Cambridge, Massachusetts 02139.*

ABSTRACT A series of light scattering experiments have been performed to study both macroscopic aspects of band formation and propagation and microscopic motility parameters of *Escherichia coli* in the combined substrate gradients of oxygen and serine. From the band formation experiment the conclusion is drawn that a minimum threshold gradient of the substrate is required for bacteria to form a band. From the band propagation experiment in the serine substrate the motility coefficient μ and chemotactic coefficient δ are determined. A separate quasi-elastic scattering experiment has been made with a propagating band to obtain three microscopic motility parameters: mean twiddle time τ_1, mean run time τ_2, and mean run speed V_2. Finally, a scaling argument is made to connect the macroscopic parameters μ and δ with the microscopic parameters τ_1, τ_2, and V_2, thus achieving a unified understanding of macroscopic and microscopic aspect of chemotaxis.

INTRODUCTION

In three previous papers (1, 2, 3) we reported on studies of one dimensional upward migration of a band of *Escherichia coli*. The bacteria form a sharp band in a cuvette containing a motility buffer saturated with oxygen when they were initially layered at the bottom. We measured the averaged motility parameters of individual bacterium within the "chemotactic band" using a newly developed small angle quasi-elastic light scattering technique. The phenomenon of band formation is intimately related to the phenomenon of chemotaxis of bacteria, i.e., the sensing of a chemical gradient of the substrate (in this case, oxygen) and a resultant collective migration in the direction of the gradient (4, 5). Macroscopically, the diffusion of substrate and the substrate consumption by bacteria combine to generate a travelling substrate concentration gradient, which the bacteria follow collectively. This collective motion results in formation of a travelling band that we called a chemotactic band. Microscopic motion of a bacterium within a band can be described as a biased random walk (6, 7, 8, 9, 10). The bacterial motion is biased toward the chemical gradient by lowering the frequency of twiddle when it is moving in that direction. In a favorable direction a bacterium tends to run longer and twiddle less frequently. As a result the bacteria on the average acquire a net drift velocity in the direction of the gradient.

In this paper we report new results when two substrates, both attractants, are present. When L-serine is added to a motility buffer which is saturated with oxygen, two chemotactic bands may be formed. Whether *E. coli* will form one or two bands depends on the relative concentrations of oxygen and L-serine (see Figs. 1 and 2). *E. coli* can consume L-serine either aerobically or anaerobically. The saturated oxygen concentration at room temperature is 2×10^{-4}M. If the L-serine concentration is more than 5×10^{-3}M, only one band is formed. This is an oxygen limited band. The bacteria consume all the oxygen and part of the L-serine and follow the gradient up to the top of the solution where the oxygen concentration is high. Since there is too much L-serine in the buffer, for the number of bacteria inoculated, the bacteria can never consume all the L-serine locally. This implies that the diffusion rate of L-serine is faster than the bacterial L-serine consumption rate. If the L-serine concentration is between 7×10^{-4}M and 5×10^{-3}M, two bands are formed and the second band (denoted as the L band) is an L-serine limited band. In the first band, bacteria use up all the oxygen and part of the L-serine. This first band follows the combined oxygen and L-serine gradients upwards. Bacteria behind the first band use L-serine anaerobically and create a L-serine concentration gradient. This second band follows the L-serine concentration gradient. If the L-serine concentration is between 3×10^{-4}M and 6×10^{-4}M, there is only one band. This is because bacteria use up all of the L-serine and oxygen simultaneously. For the cases where the L-serine concentration is less than 1×10^{-4}M, there are two bands

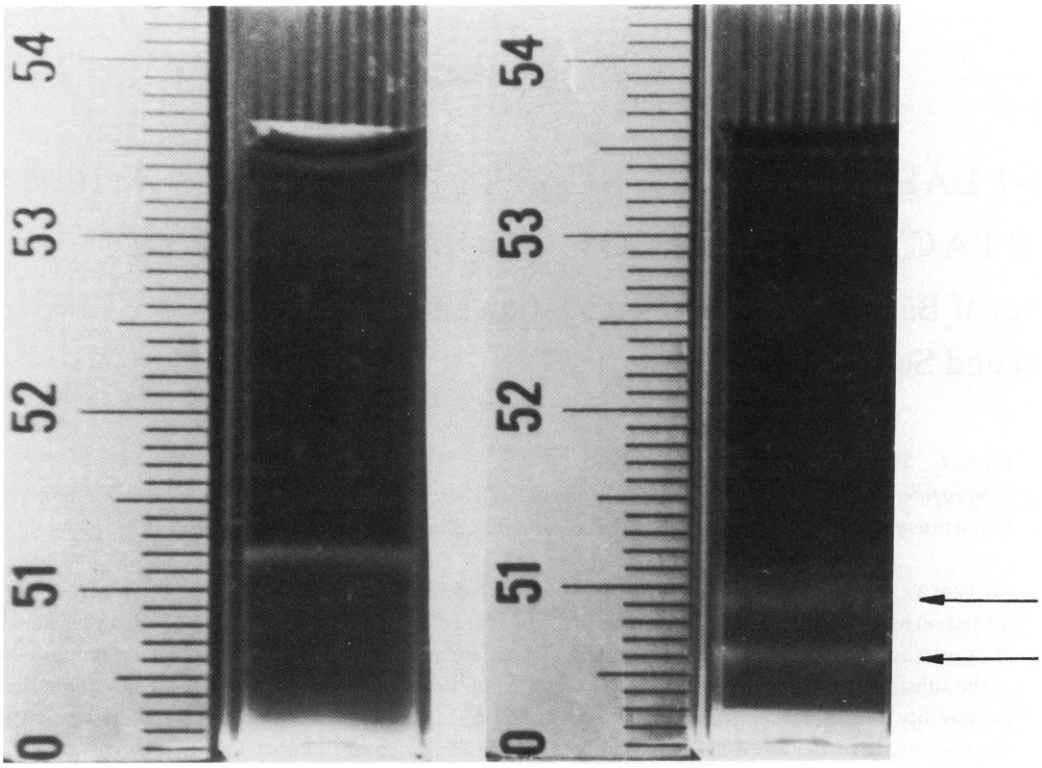

FIGURE 1 Two examples of chemotactic bands in serine solution. The figure on the right was taken 1,800 s after the inoculation in a solution containing 8×10^{-4}M of serine. The top band is a combined serine-oxygen band and the bottom one is a pure serine band. The figure on the left was taken 330 s after the inoculation in a solution containing 3×10^{-4} serine. There is only one band because the serine concentration is approximately equal to the equilibrium oxygen concentration $C_0 = 2 \times 10^{-4}$M.

again. In these cases the first band is L-serine-limited and the second band is oxygen-limited.

First, we present a study of the initial stage of band formation which indicates that a minimum substrate concentration gradient is required for bacteria to be able to form a chemotactic band. This "threshold" gradient can be expressed in terms of a minimum chemotactic speed, V_c, and we give values of V_c for two plausible models of chemotaxis. We then present results for propagation of a serine band where the motility coefficient μ and chemotactic coefficient δ are determined for the serine substrate. As a continuation and extension of a previous work (3) we reformulate the theory of the photon correlation function in the two-state model taking into account migration of the band and show that slow migration of the band has a negligible effect on measurements of the photon correlation function along the direction of the gradient. An improved analysis of the small angle quasielastic light scattering spectrum is then made taking into account both heterodyne and homodyne contributions. The microscopic motility parameters are extracted from the measurements taken from the serine band. Finally, we present a scaling argument which relates the macroscopic parameters μ and δ and the microscopic motility parameters measured by quasielastic light scattering, thus bridging the theories based on two levels of description.

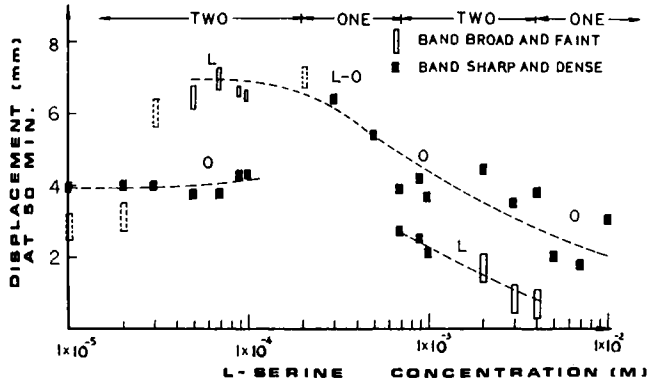

FIGURE 2 Positions of chemotactic bands in oxygen saturated serine solutions 50 min after inoculation. L stands for s serine band and O stands for an oxygen band. Between serine concentrations of 3×10^{-4} to 6×10^{-4}M there is only one serine-oxygen band. The dashed line blocks represent the top positions of the bands that had diffused away at the time the data was taken.

STUDY OF BAND FORMATION

Interaction between bacterial density and substrate concentration gives rise to a macroscopic manifestation of chemotaxis. For simplicity an experimental condition was chosen in such a way that the chemotactic motion was one-dimensional. Bacteria initially were layered on the bottom of a cuvette in which there was a buffer with a uniform distribution of substrate concentration. As bac-

teria started to consume substrate they created a substrate concentration gradient. Some of the bacteria follow this self-created substrate concentration gradient to form a travelling band.

A phenomenological mathematical model was first proposed by Keller and Segel (KS) (11) to describe this macroscopic aspect of chemotaxis. There are two continuity equations expressing the conservation of bacteria $b(z,t)$ and substrate $C(z,t)$.

$$\frac{\partial b(z,t)}{\partial t} = -\frac{\partial}{\partial z}\left[-\mu\frac{\partial b(z,t)}{\partial z} + V_c(C)b(z,t)\right] \quad (1)$$

$$\frac{\partial C(z,t)}{\partial t} = -\frac{\partial}{\partial z}\left[-D\frac{\partial C(z,t)}{\partial z}\right] - k(C)b(z,t), \quad (2)$$

where b and C are the bacterial density and substrate concentration. The first term in the bracket on the right hand side of Eq. 1 expresses a diffusion current due to the random motion. μ is the motility coefficient. The second term is the effective chemotactic current where V_c is a net drift velocity. In the substrate conservation equation, Eq. 2, D is the diffusion coefficient of the substrate in the buffer, and $k(C)$ is the number of substrate molecules consumed per second per bacteria. Eqs. 1 and 2 are valid only when the average distance between two bacteria is longer than the mean free path of the bacterial run motion between turns.

A "sensitivity" function $f(C)$ was introduced by Keller and Segal (7) and others (12, 13) to link the chemotactic velocity V_c with the substrate gradient $\partial C/\partial z$. V_c is assumed to be linearly proportional to the spatial differentiation of $f(C)$, i.e.,

$$V_c = \delta \mathrm{d}f(C)/\mathrm{d}z, \quad (3)$$

where $\delta(\mathrm{cm}^2/\mathrm{s})$ is the chemotactic coefficient. $\mathrm{d}f(C)/\mathrm{d}z$ is an indicator of the strength of chemotaxis. Based on a well-known Weber-Fechner law of sensation (14), Keller and Segal (KS model) proposed that f equals $\ell\mathrm{n}C/C_{th}$, where C_{th} is the threshold concentration for bacteria to have chemotactic responses. V_c is then equal to $(\delta/C)\partial C/\partial z$. Considering equilibrium binding and dissociation of the protein receptors and chemoeffectors, Mesibov and coworkers (12) derived an expression for f by equating it to the fraction of bounded receptors, i.e., $f = C/(C + k_d)$. k_d is the dissociation constant of receptor-chemoeffector complex. Following this, Lapidus and Schiller (13) proposed a model (LS model) that V_c is $\delta k_d C(\partial C/\partial z)/(C + k_d)^2$. These two different models lead to predictions of different initial drift velocities and steady state bacterial density distributions.

Keller and others (11, 15) have made attempts to solve these two governing equations either numerically or analytically under some specific conditions. They focused attention on solutions applicable to the initial formation and subsequent propagation of the band with a constant migration speed. In order to compare different predictions based on the KS model and the LS model we solve Eqs. 1 and 2 analytically for the two respective models corresponding to the initial band formation situation. We also carry out light-scanning experiments to monitor the development of a band. From comparison of the theory and the experiments we draw a conclusion on the existence of a threshold substrate gradient below which chemotaxis would not occur.

To solve for the initial stage of the band formation analytically, we assume that the bacteria density does not change appreciably during a time interval in which we are interested. Existence of such a time interval is possible because for an oxygen substrate, the diffusion rate of the substrate is much faster than the diffusion rate of the bacteria. In fact using $D = 2.12 \times 10^{-5}\ \mathrm{cm}^2/\mathrm{s}$, it was shown that both μ/D and δ/D are of the order of 0.1 (2). During this time interval, the bacterial density is constant from the bottom of the cuvette to the top of the inoculum. We can then solve for the substrate concentration and its derivatives as functions of positions at different times. From the spatial derivatives of substrate concentration, chemotactic velocities can be calculated, provided that the fraction of the bacteria which move out from the original location is known.

If the inoculum region and the rest of the cuvette are considered as two separate regions, then this problem can be formulated as follows (16):

$$\text{in inoculant region I: } \frac{\partial C_I}{\partial t} = D\frac{\partial^2 C_I}{\partial z^2} - kb_0, \quad (4)$$

$$\text{in the buffer region II: } \frac{\partial C_{II}}{\partial t} = D\frac{\partial^2 C_{II}}{\partial z^2}, \quad (5)$$

b_0 is the original bacteria density. The boundary conditions are

at $z = 0$,

$$\frac{\partial C_I}{\partial z} = 0 \quad (6)$$

at $z = z_0$,

$$C_I(z_0, t) = C_{II}(z_0, t) \quad (7)$$

$$\frac{\partial C_I(z,t)}{\partial z} = \frac{\partial C_{II}(z,t)}{\partial z} \quad (8)$$

and $z = \infty$,

$$C_{II}(z, t) = C_0. \quad (9)$$

The initial condition is

$$t = 0,\ C(z,0) = C_0. \quad (10)$$

Eq. 6 shows the cuvette is closed at the bottom. Eq. 9 means the buffer extends to infinity as far as the bacteria in the inoculum are concerned. The initial substrate concentration is constant, C_0, throughout the cuvette. Eqs. 7

and 8 show that substrate concentration and its derivative are continuous at the boundary z_0. Eqs. 4 and 5 are then solved rigorously by a Laplace transformation method (17). The solutions are

$$\tilde{C}_{\mathrm{I}} = 1 - \tilde{t} + \frac{1}{2}\left[\left(\tilde{t} + \frac{(1-\tilde{z})^2}{2\tilde{D}}\right) Erfc\left(\frac{(1-\tilde{z})}{2\sqrt{\tilde{D}\tilde{t}}}\right) + \left(\tilde{t} + \frac{(1+\tilde{z})^2}{2\tilde{D}}\right) Erfc\left(\frac{(1+\tilde{z})}{2\sqrt{\tilde{D}\tilde{t}}}\right) - \sqrt{\frac{\tilde{t}}{\pi\tilde{D}}}(1-\tilde{z}) \exp\left(-\frac{(1-\tilde{z})^2}{4\tilde{D}\tilde{t}}\right) - \sqrt{\frac{\tilde{t}}{\pi\tilde{D}}}(1+\tilde{z}) \exp\left(-\frac{(1+\tilde{z})^2}{4\tilde{D}\tilde{t}}\right)\right] \quad (11)$$

$$\tilde{C}_{\mathrm{II}} = 1 - \frac{1}{2}\left[\left(\tilde{t} + \frac{1}{2}\frac{(\tilde{z}-1)^2}{\tilde{D}}\right) Erfc\left(\frac{(\tilde{z}-1)}{2\sqrt{\tilde{D}\tilde{t}}}\right) - \left(\tilde{t} + \frac{(\tilde{z}+1)^2}{2\tilde{D}}\right) Erfc\left(\frac{(\tilde{z}+1)}{2\sqrt{\tilde{D}\tilde{t}}}\right) - \sqrt{\frac{\tilde{t}}{\pi\tilde{D}}}(\tilde{z}-1) \exp\left(-\frac{(\tilde{z}-1)^2}{4\tilde{D}\tilde{t}}\right) + \sqrt{\frac{\tilde{t}}{\pi\tilde{D}}}(\tilde{z}+1) \exp\left(-\frac{(\tilde{z}+1)^2}{4\tilde{D}\tilde{t}}\right)\right] \quad (12)$$

$$\frac{d\tilde{C}_{\mathrm{I}}}{d\tilde{z}} = \sqrt{\frac{\tilde{t}}{\pi\tilde{D}}}\left[\exp\left(-\frac{(1-\tilde{z})^2}{4\tilde{D}\tilde{t}}\right) - \exp\left(-\frac{(1+\tilde{z})^2}{4\tilde{D}\tilde{t}}\right)\right] + \frac{1}{2\tilde{D}}\left[(1+\tilde{z})\, Erfc\left(\frac{1+\tilde{z}}{2\sqrt{\tilde{D}\tilde{t}}}\right) - (1-\tilde{z})\, Erfc\left(\frac{1-\tilde{z}}{2\sqrt{\tilde{D}\tilde{t}}}\right)\right] \quad (13)$$

$$\frac{d\tilde{C}_{\mathrm{II}}}{d\tilde{z}} = \sqrt{\frac{\tilde{t}}{\pi\tilde{D}}}\left[\exp\left(-\frac{(\tilde{z}-1)^2}{4\tilde{D}\tilde{t}}\right) - \exp\left(-\frac{(\tilde{z}+1)^2}{4\tilde{D}\tilde{t}}\right)\right] + \frac{1}{2\tilde{D}}\left[(\tilde{z}+1)\, Erfc\left(\frac{\tilde{z}+1}{2\sqrt{\tilde{D}\tilde{t}}}\right) - (\tilde{z}-1)\, Erfc\left(\frac{\tilde{z}-1}{2\sqrt{\tilde{D}\tilde{t}}}\right)\right]. \quad (14)$$

These solutions are presented in a dimensionless form in order to be compared with any experimental results. The dimensionless variables are

$$\tilde{z} = \frac{z}{z_0},\ C_{\mathrm{I,II}} = \frac{C_{\mathrm{I,II}}}{C_0},\ \tilde{t} = \frac{t}{\tau},\ D = \frac{D\tau}{z_0^2},\ \tau^{-1} = \frac{kb_0}{C_0}, \quad (15)$$

where z_0 is the height of the inoculum, 0.25 cm is used in this computation. C_0 is the saturated substrate concentration. For oxygen in water at room temperature C_0 is 2×10^{-4}M. D is the oxygen diffusion constant which is taken to be 2×10^{-5}cm^2/s. The bacterial density, b_0, is 10^8/ml. τ equals 1,400 s. These dimensionless solutions of $\tilde{C}$ as functions of $\tilde{z}$ are also presented in graphic form in Fig. 3. The depletion of the substrate and the formation of the substrate gradient are clearly demonstrated in Fig. 3. Fig. 4 is the chemotactic speec, V_c, derived from the KS model. Fig. 5 is V_c derived from the LS model. $\bar{\delta}$ is taken to be 2 in the calculation. These graphs may be used to determine the threshold chemotactic speed for a given experimental condition. For example, we generally find that 10% of the bacteria from the inoculum formed a band. We can therefore draw a line at $\tilde{z} = 0.9$ and the intersections would give the chemotactic speeds at different times. Suppose we experimentally observe that the band formed in 2 min

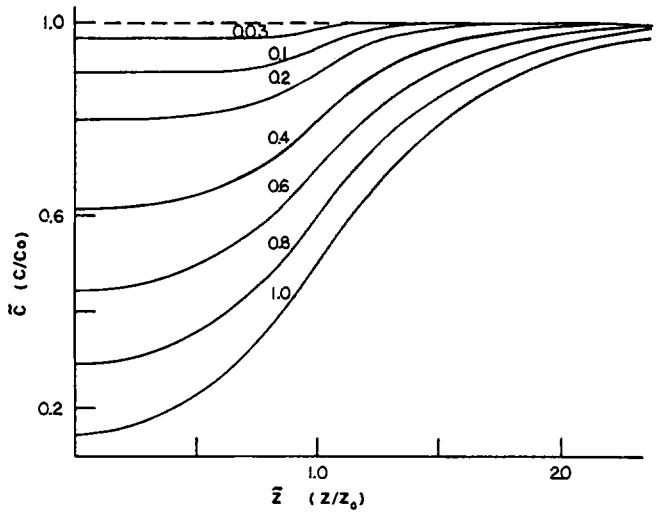

FIGURE 3 Theoretical curves of dimensionless substrate concentration $\tilde{C}$, computed by Eq. 11 and 12, as function of positions at different time. The inoculant height z_0 is 0.25 cm. The saturated substrate concentration C_0 is 2×10^{-4} M. The numbers on each curve are the dimensionless time. The diffusion constant D is taken to be 2×10^5 cm^2/s. b_0, the bacteria density, is 10^8/ml.

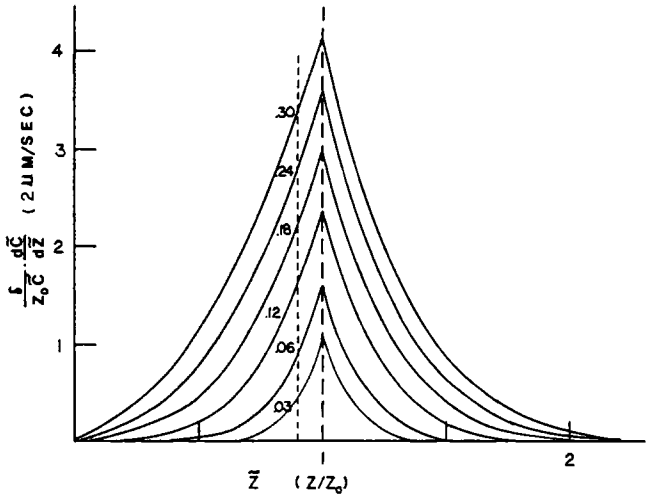

FIGURE 4 Chemotactic speed V_c derived from the KS model according to $V_c = \delta df/d\tilde{z}$, where $f = \ln \tilde{C}/\tilde{C}_{\mathrm{th}}$. Theoretical values of V_c can be read out directly if the fraction of the bacteria that move out is known. For example, if 10% of the bacteria move out to form a band then we draw a dashed line at $\tilde{z} = 0.9$, the cross point gives $V_c = 1.0$ μm/s at $\tilde{t} = 0.045$.

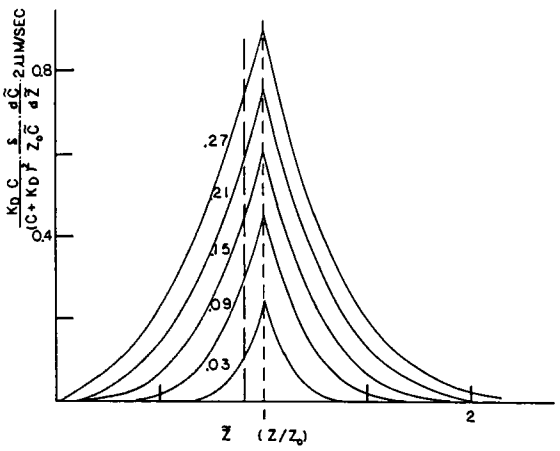

FIGURE 5 Chemotactic speed V_c derived from the LS model according to Eq. 4. If 10% of bacteria move out to form a band, then the corresponding V_c is 0.24 μm/s at $\tilde{t}$ = 0.045, which is 1 min after inoculation in real time.

($\tilde{t}$ = 0.09) after inoculation, then intersections of the $\tilde{z}$ = 0.9 line with the V_c curves for the $t < 2$ min would give us the minimum chemotactic speed, V_c, required for the bacteria to move out and form a band. If t is taken to be 1 min ($\tilde{t}$ = 0.045), the intersections are 0.5 in Fig. 4 and 0.12 in Fig. 5. After conversion, the corresponding chemotactic speeds are 1.0 μm/s for the KS model, and 0.24 μm/s for the LS model. In view of the initial band migration speed of 1 μm/s, both these threshold speeds seem to be reasonable. The band formation process and its propagation are recorded by a densitometer. The bacterial density distribution as a function of time are shown in "Study of Band Propagation."

STUDY OF BAND PROPAGATION

A light-scanning setup similar to that of Holz (2) was used to map out the band profiles as functions of time. When a migrating chemotactic band passes through a stationary laser beam, the intensity of 90° scattered light is proportional to the bacterial density in the scattering volume. The scattered light is detected by a photomultiplier. The output of the photomultiplier is amplified and shaped into logic pulses which are then fed to the input of a multichannel analyzer (MCA). By repeatedly recording the scattered light intensities from the MCA, the chemotactic band profiles as functions of time are then obtained. Positions of the band peaks as functions of time are recorded from a sequence of band profiles. The migration velocity is then computed. From the profiles, we can also determine how many bacteria move out to form a band. The lowest point in a profile is taken to be the boundary of a band. The bacteria density is calculated from the initial inoculum density and its corresponding scattered light intensity. The area under the peak of a profile gives the total number of bacteria in the band. All of our experiments show that ~9 to 13% of bacteria from the inoculant move out to form a band. The number of bacteria in the band stays constant for a long time and gradually decreases because of bacterial diffusion (18). At that time, the band migration slows down.

E. coli K12 wild type bacteria were grown in L-broth to mid-log phase at 37°C aerobically. The bacterial density was 5×10^8/ml in the inoculant. The bacterial density in the chemotactic band gradually decreased to 10 to 20% of its original value as the band moved out. This lower density situation satisfies the validity condition of Eqs. 1 and 2 that the average distance between two bacteria is longer than the mean free path of bacterial run motions. A scattering cuvette (square section = 9 mm^2) was rinsed and filled with a motility buffer that contains 8×10^{-4}M L-serine. 70 μl of the culture medium was carefully layered at the bottom of a cuvette. The inoculant height was ~8 mm. The starting point of scanning was adjusted to be 3 mm below the top of the inoculant. This assured that in every scan the band as well as some part of the original inoculant were scanned through. By doing so, the band positions had a reference point and the bacterial density of the inoculant could be monitored. Fig. 6 shows the band profiles in a case where two bands are formed. The first is oxygen-limited and the second is L-serine-limited. The second band is formed about 11 min after inoculation. The bacterial density decreased with time. This lagging behind of the bacteria alters the process of generation of the substrate concentration gradient, because the total substrate consumption rate is lower for fewer bacteria. The shallower concentration gradient reduces the chemotactic effect. Fig. 7 is the peak positions of both the oxygen and serine-limited bands. The migration speed of the oxygen-limited band is 3.4 μm/s and for the serine-limited band it is 2.9 μm/s.

The motility coefficient μ and chemotactic coefficient δ are the two most important macroscopic quantities describing chemotaxis. In the oxygen case, these coefficients can be extracted from the band shape using a moment analysis method (2). Using the same method we carefully analyzed the second band in 8×10^{-4} M L-serine case. This is a pure L-serine-limited band. Thus the δ and μ values for *E. coli* in serine are obtained. The fifth picture in Fig. 6 is used for this analysis. Holz and Chen (2) first solve Eqs. 1 and 2 numerically for different combinations of the $\bar{\delta}$ and γ values. $\bar{\delta}$ is defined as δ/μ and γ is μ/D. They get a theoretical distribution function $b(x)/b_{max}$ for every set of $\bar{\delta}$ and γ. The moments of these theoretical distribution functions are compared with the moments of the experimental bacterial distribution function, and $\bar{\delta}$ and μ are thus extracted. For the serine band $\bar{\delta}$ is 3.18 and μ is 3.79×10^{-6} cm^2/s.

STUDY OF MOTILITY IN THE PRESENCE OF A SUBSTRATE GRADIENT

The dynamic parameters of microscopic bacterial motion in a chemotactic band can be obtained from a small angle

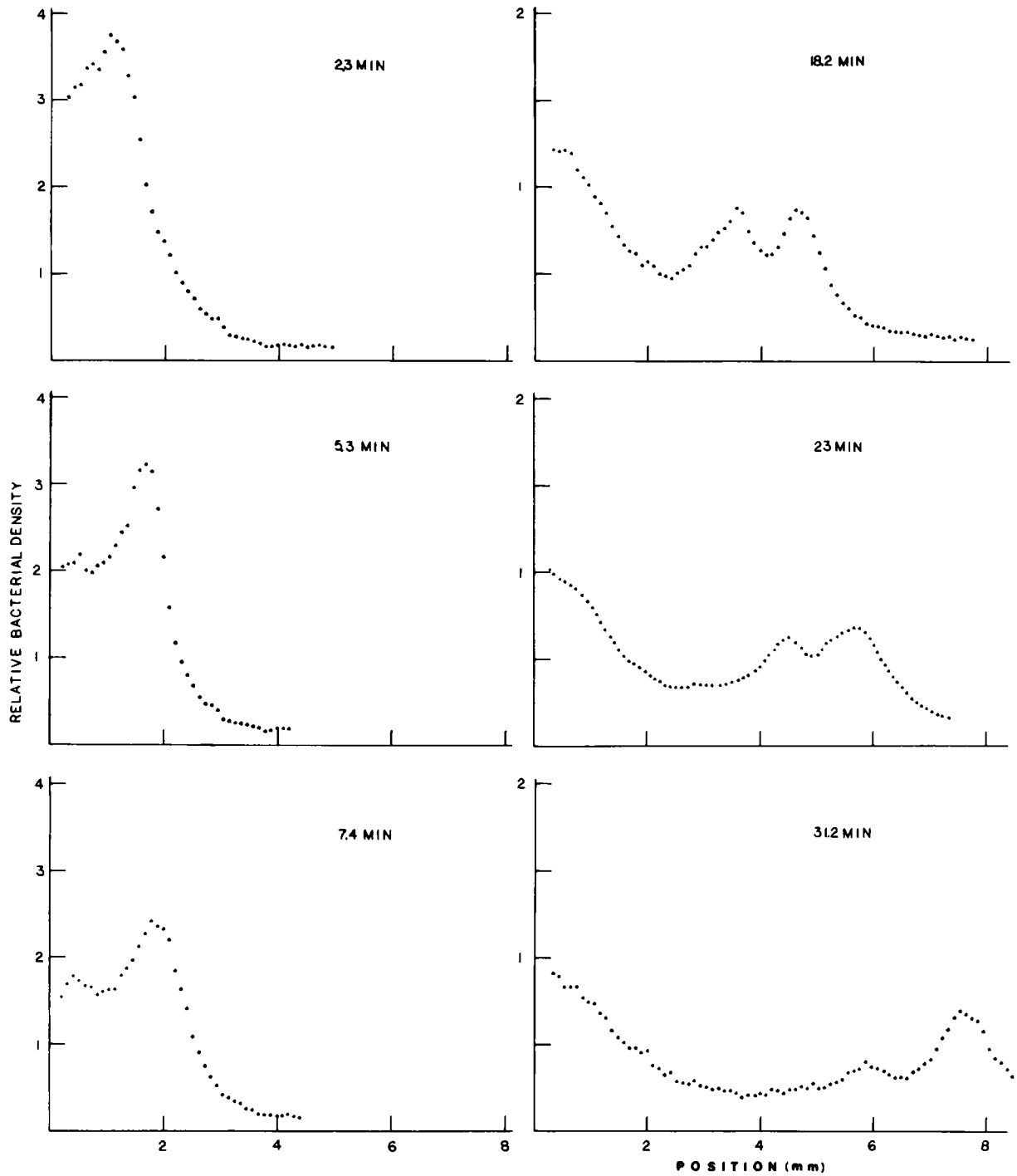

FIGURE 6 Formation of two bands. Additional 8×10^{-4}M L-serine was added to the buffer as an attractant. The second band, which is serine limited, was formed 10–15 min after inoculation. The relatively low bacteria densities for these bands at later times show that the bands gradually become weaker.

laser light scattering technique (3, 19). In this section, we present an improved theory taking into account the net chemotactic drift velocity in the direction of the gradient. Experimentally, we used an improved light chopping method to measure the photon correlation function in both parallel and perpendicular directions simultaneously.

Improved Theory of Anisotropic Motion

In the photon correlation technique (20) the measured photo-count correlation function is reducible to the self-correlation function

$$F_s(q, t) = \langle e^{iq[R(t)-R(0)]} \rangle, \quad (16)$$

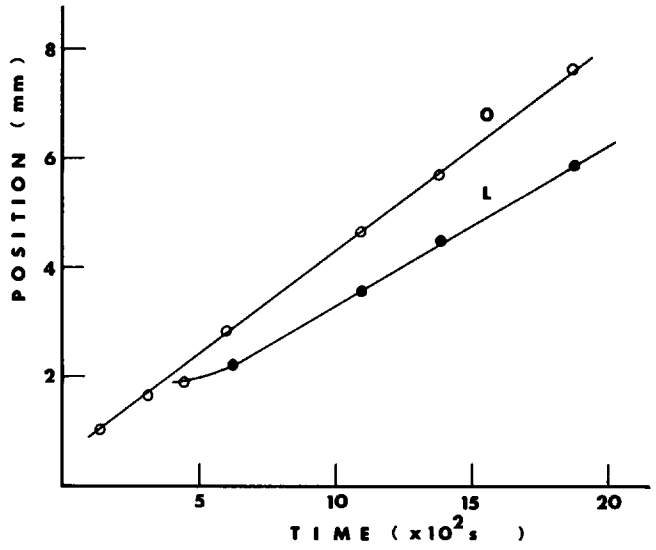

FIGURE 7 The peak positions of the oxygen and serine bands from Fig. 6. The dotted section indicates the formation of the second band. The top line indicates positions of the oxygen band at various times. The migration speed is 3.4 μm/s. The second line indicates the positions of the serine band at various times. Its migration speed is 2.9 μm/s.

where $R(t)$ and $R(0)$ are the position vectors of a typical bacterium at time t and 0, respectively. Time 0 is an arbitrarily chosen time origin. $q = (4\pi/\lambda)n \sin(\theta/2)$ is the magnitude of the scattering vector, in terms of the wavelength of the laser light λ. n is the index of refraction of the medium and θ is the scattering angle. For a small scattering angle $\theta < 5°$, and the typical dimension of *E. coli* $d \sim 1 \times 10^{-4}$cm, $qd < 1$. For data taken at this small scattering angle we can safely treat an *E. coli* as a point particle and model only its center of mass motion.

In a homogeneous medium where motions are isotropic, $F_s(q, t)$ depends only on the magnitude of $\vec{q}$. On the other hand, when motions are not isotropic, such as in the case of bacteria in a chemotactic band, $F_s(q, t)$ depends on the direction of the $\vec{q}$ vector also. Let us take the direction of the oxygen gradient (vertical direction) as the z-direction and the direction perpendicular to it as the x-direction. Then we have

$$F_{\parallel}(q, t) = \langle e^{iq[z(t)-z(0)]} \rangle, \tag{17}$$

$$F_{\perp}(q, t) = \langle e^{iq[x(t)-x(0)]} \rangle. \tag{18}$$

Since the origin of time is arbitrary, we determine $Z(t) = z(t) - z(0)$ and $X(t) = x(t) - x(0)$.

Free Motion. For bacteria in the run state, we can set $z(t) = v_z t$ for the motion in the z-direction and thus

$$F_{\parallel}(q, t) = \langle e^{iqv_z t} \rangle = \langle e^{iqv\cos\theta} \rangle =$$

$$\int_0^{\infty} \int_{-1}^{1} \int_0^{2\pi} e^{iqvt\cos\theta} p(v) p(\cos\theta) p(\varphi) v^2 dv d(\cos\theta) d\varphi, \tag{19}$$

where V is the bacterial run speed. It has been shown by a direct optical tracking of *E. coli* (21) in an isotropic medium that the speed distribution is closely approximated by a Maxwell distribution for which

$$p(v) = (2\pi V_2^2)^{-3/2} \exp(-v^2/2V_2^2), \; p(\varphi) = p(\cos\theta) = 1, \tag{20}$$

where V_2 is an experimentally determined averaged bacterial run speed. Substituting Eq. 20 into Eq. 19 we get, for an isotropic substrate distribution

$$F_{\parallel}(q, t) = \exp(-q^2 V_2^2 t^2/2). \tag{21}$$

We can also determine the average speed $\langle v \rangle = (8/\pi)^{1/2} V_2$, drift velocity $\langle v_z \rangle = 0$ and $\langle v_z^2 \rangle = V_2^2$. With a simple integration $F_{\perp}(q, t)$ in the x direction can also be written in the same form as Eq. 21 with the same $\langle v \rangle$, $\langle v_x \rangle$ and $\langle v_x^2 \rangle$ values.

In a chemotactic situation, we assume that the speed distribution $p(v)$ and the azimuthal distribution $p(\varphi)$ are the same as in the isotropic case. However, the angular distribution $P(\cos\theta)$ may be approximated as $p(\cos\theta) = 1 + \Delta \cos\theta$, where Δ is a small dimensionless quantity.

It can easily be shown, using this new velocity distribution, that $\langle V_x \rangle = \langle V_y \rangle = 0$, $\langle V_z \rangle = \frac{1}{3}\Delta\langle V \rangle$ and $\langle v_x^2 \rangle = \langle V_y^2 \rangle = \langle V_z^2 \rangle = V_2^2$. These results show that although bacteria maintain the same rms speed as in the isotropic case, they now have a net drift velocity, $\frac{1}{3}\Delta\langle V \rangle$, in the z-direction. One can estimate the dimensionless quantity, Δ, by equating the experimental band imigration speed, $\bar{v}$, to $\langle v_z \rangle$,

$$\bar{v} = \tfrac{1}{3}\Delta\langle V \rangle. \tag{22}$$

Since $\bar{v} \sim 1$ μm/s, $\langle V \rangle \sim 20$ μm/s, Eq. 22 gives $\Delta \sim 0.15$. In this case the correlation functions are

$$F_{\parallel}(q, t) = \exp[-q^2 V_2^2 t^2/2] + i\Delta\langle j_1(qvt) \rangle, \tag{23}$$

$$F_{\perp}(q, t) = \exp[-q^2 V_2^2 t^2/2]. \tag{24}$$

The correlation function in the perpendicular direction is the same as in the isotropic case, but in the parallel direction there is a small correction due to band drifting. $j_1(qvt)$ is a spherical Bessel function of the first kind. In a homodyne case one measures

$$|F_{\parallel}(q, t)|^2 = \exp[-q^2 V_2^2 t^2] + \Delta^2 |\langle j_1(qVt) \rangle|^2, \tag{25}$$

while in a heterodyne case, one measures

$$Re\, F_{\parallel}(q, t) = \exp[-q^2 V_2^2 t^2/2]. \tag{26}$$

In this calculation, the effects of the band drift due to chemotaxis are included. This is an improvement over our previous model. This modification gives an additional term $\Delta^2 |\langle j_1(qvt) \rangle|^2$ in homodyne measurements. However, it does not enter into a heterodyne measurement because in this case only the real part of the self correlation function enters. In our *E. coli* aerotaxis band migration experiment,

the drift velocity $\langle v_z \rangle = 0.8\ \mu m/s$, and $V_2 = 14\ \mu m/s$, and the correction term in Eq. 25 is only ~1%.

The free motion approximation is good when the mean free path of the free motion L_2 is larger than q^{-1}. For example, a typical run L_2 may be 20 μm and this criterion is amply satisfied for q values at all attainable scattering angles.

Short Step Motion: Gaussian Approximation. *E. coli* in the twiddle state can be modeled as a series of small step motions, as far as the center of mass motion is concerned (1). When the change of direction is so rapid that $qL_1 < 1$ then the motion can be modeled as a random walk of step length L_1. This is a Gaussian random process and a well-known theorem (22) states

$$F(q,t) = \langle e^{iqZ(t)} \rangle = \exp(-q^2\langle Z^2(t)\rangle/2) = \exp(-q^2 D_E t), \quad (27)$$

where D_E is the equivalent diffusion constant of the twiddle motion.

The total self-correlation function can be written as (3)

$$F_s(q,t) = \frac{\tau_1}{\tau_1+\tau_2} P_{run}(t)\, F_{run}(q,t) + \frac{\tau_2}{\tau_1+\tau_2} P_{tw}(t)\, F_{tw}(q,t) + \frac{2}{\tau_1+\tau_2}\int_0^t dt_1 P_{run}(t-t_1) P_{tw}(t_1)\, F_{run}(q,t-t_1)\, F_{tw}(q,t_1) + \text{higher order terms}, \quad (28)$$

where F_{run} and F_{tw} are the correlation functions of free and short step motions. τ_1 and τ_2 are the average run and twiddle times. The third term is the contribution from the bacteria that make one transition, either from run to twiddle or from twiddle to run, during the period of observation. If the observation time t (the decay time of the correlation function) is small compared with both τ_1 and τ_2, then during the observation the majority of bacteria can make at most only one transition. We can therefore safely neglect the higher-order terms.

EXPERIMENTAL SET-UP

An improved laser light scattering technique (Chao, Y. S., P. C. Wang, and S. H. Chen, manuscript submitted for publication.) similar to our previous studies (19) using a small angle geometry is introduced. The scattered light is projected onto a screen with two pinholes, one in the vertical direction and one in the horizontal direction. This way the scattering vector can be chosen to be either in the vertical or in the horizontal direction. Light passes through the pinholes and is focused upon the photocathode of a photomultiplier. The magnitude of the scattering vector is determined by the pinhole position and the distance from the scattering volume to the pinhole. The scattering angle is adjustable; three angles, 2.5°, 3.0°, and 3.5° are used in the experiment. A mask is driven up and down by a motor. It blocks one of the two pinholes alternately. These up and down motions are synchronized with the start function of the multi-channel analyzer (MCA) so that the measured photon correlation functions in the two directions can be stored in two different quarters of the MCA. Each quarter has 256 channels. This pin-hole geometry insures that the measured scattered light comes from the same scattering volume, thus removing the ambiguity of whether the scattered light for the two different scattering vectors is from the same region of the chemotactic band. The methods of signal processing, computer control, data storing on cassette tape and extracting the self-correlation functions are the same as in our previous studies (19). With this newly incorporated chopping apparatus and the synchronization of the MCA to the chopping motion, the photon correlation functions in both perpendicular and parallel directions are measured simultaneously.

The experimental conditions for the formation of oxygen and serine bands have been described in "Study of Band Propagation." Two correlation functions (see Fig. 8) at the center of the serine band in both directions are carefully analyzed according to the improved theory of anisotropic motion in Eq. 28.

In this series of experiments there is always some heterodyne signals mixed in with homodyne signals being measured. The normalized photon correlation functions can be written as (23)

$$\frac{\langle n(0)n(t)\rangle - B}{\langle n(0)n(0)\rangle - B} = \alpha f(A) Re F_s + (1-\alpha) f'(A) |F_s|^2, \quad (29)$$

where

$$\alpha \equiv \frac{2\langle n_L\rangle\langle n_s\rangle}{2\langle n_L\rangle\langle n_s\rangle + \langle n_s\rangle^2}. \quad (30)$$

$n(t)$ is the number of photon counts detected. $\langle n_s \rangle$ and $\langle n_L \rangle$ stand for photon counts per sampling time of scattered and unscattered light, respectively. The ratio of $\langle n_s \rangle / \langle n_L \rangle$ is related to signal-to-background ratio as follows:

$$\frac{\langle n_s\rangle}{\langle n_L\rangle} = \left(1 - \frac{C_0 - B}{B}\right)^{-1/2} - 1, \quad (31)$$

where C_0 is the photon count at channel zero and B is the background. Using Eq. 30 and 31 α can be calculated from a given signal-to-background ratio. $f(A)$ and $f'(A)$ are coherence factors that depend on the optical geometry of the set up. In this experiment, $f(A)$ is 0.9 and $f'(A)$ is taken as the same as $f(A)$. F_s is the total correlation function as

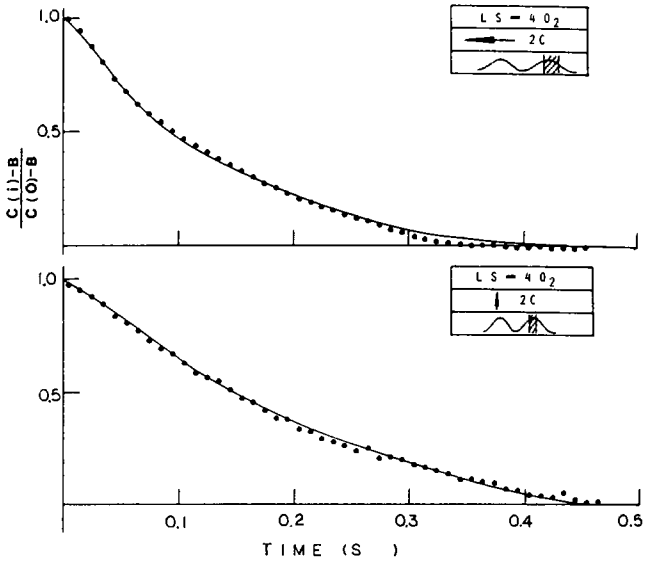

FIGURE 8 Normalized scattered light intensity correlation functions taken from the center of a serine band. The L-serine concentration 8×10^{-4}M, four times that of the saturated oxygen concentration. The solid lines are the fitted curves according to Eq. 29. The fitted results are in Table I.

given in Eq. 28, which contains both real and imaginary parts. The microscopic parameters of bacterial motions extracted by this method are listed in Table I. This table shows that in a direction parallel to that of the traveling band, bacteria tend to run for a longer time, that is, relatively less bacteria are in the twiddle state (smaller β). The equivalent diffusion constants, D_E, for twiddle motions are the same in both directions. V_2 is related to the average run speed by $\langle V \rangle = 1.6\ V_2$. Even though V_2 is slightly smaller in the parallel direction, because of a considerably smaller value of β the mean square displacement $\langle Z^2 \rangle$ is larger than $\langle X^2 \rangle$ at all times as was shown in reference 3.

RELATION BETWEEN MICROSCOPIC AND MACROSCOPIC PARAMETERS

In the KS theory the macroscopic description of chemotaxis is based on two parameters, the motility coefficient μ and the chemotactic coefficient δ. On the other hand, in microscopic description the most important parameters are μ, the twiddle time τ_1, the run time τ_2 and the run speed V_2. Theoretically, these two sets of parameters should be related. Experimentally, we performed both scanning and small-angle light scattering experiments to measure these parameters. These parameters are connected in a dimensional analysis by writing a generalized model of chemotaxis as follows:

$$\text{response} = \int_{\text{sensing time}} (\text{signal}) dt. \tag{32}$$

By a tracking microscope technique, Berg and Brown (6, 24, 25) have shown that there is a run distance increase, ΔL, in the direction of the gradient. Therefore, the response can be written as $\Delta L/L$, where L is the run distance in a homogeneous medium. Mesibov (12) and others argued that the chemotactic response is a function of the change in receptor occupancy over a period of signal processing time. The signal processing time should be of the order of run time, τ_2. Eq. 32 then becomes

$$\frac{\Delta L}{L} = A \int_0^{\tau_2} \frac{df}{dt} dt. \tag{33}$$

A is a proportional constant, which is of the order of unity. If we identify ΔL and L in terms of the effective chemotactic speed V_c and the mean run speed $\langle V \rangle$ as: $V_c \tau_2 = \Delta L$ and $\langle V \rangle \tau_2 = L$. Then from Eq. 33 we get

$$V_c = \tau_2 \langle V \rangle \overline{\frac{df}{dt}} = \tau_2 \langle V \rangle^2 \overline{\frac{df}{dz}} = \delta \overline{\frac{df}{dz}}, \tag{34}$$

TABLE I
MOTIONAL PARAMETERS OF E. COLI (K12, WILD TYPE) IN A L-SERINE GRADIENT OBTAINED BY THE RUN-TWIDDLE ANALYSIS

Position	τ_1(s)	τ_2(s)	$\beta(\tau_1/(\tau_1+\tau_2))$	$D_E(\mu m^2/s)$	$V_2(\mu m/s)$
Parallel center	0.43	0.60	0.42	18	10
Perpendicular center	0.43	0.17	0.72	18	14

where the bar is a time average and $\delta = \tau_2 \langle V \rangle^2$. The proportionality of the chemotactic coefficient δ to $\langle V \rangle^2$ has been shown previously by Segel (26) and Nossal (27).

The motility coefficient μ can be obtained from a simple kinetic theory argument:

$$\mu = \frac{1}{3} \langle V \rangle^2 (\tau_1 + \tau_2)/(1 - \overline{\cos\theta}), \tag{35}$$

where θ is the directional change between two runs. Following Berg and Brown (6) we take $\overline{\cos\theta}$ to be ~0.5. Microscopic parameters in Eq. 35 should be taken from an experiment where there is no gradient. We use data from bacteria in a homogeneous medium or from bacteria in the direction perpendicular to the gradient.

From data of the serine band in the perpendicular direction, $\tau_1 = 0.43$ s, $\tau_2 = 0.17$ s and $\langle V \rangle = (8/\pi)^{1/2} V_2 = 22.3\ \mu m/s$. From Eq. 35 we get $\mu = 2.0 \times 10^{-6}\ cm^2/s$. In the parallel direction, $\tau_2 = 0.6$ s and use $\langle V \rangle = 22.3\ \mu m/s$, $\delta = 3.0 \times 10^{-6}\ cm^2/s$, or $\bar{\delta} = 1.5$. From the macroscopic measurement, $\mu = 3.79 \times 10^{-6}\ cm^2/s$ and $\bar{\delta} = 3.18$. The agreement between the microscopic and macroscopic parameters well illustrates the connections of these two sets of parameters, at least in the sense of dimensional analysis.

CONCLUSION

In this paper a theoretical result has been presented that gives the initial-stage solutions of KS phenomenological equations for the formation of a chemotactic band. Two different chemotactic speeds, Vc, are predicted based on two sensitivity models, KS and LS models. In KS model, Vc is equal to $(\delta/C)\ \partial C/\partial z$. In LS model, Vc is equal to $\delta k_d C(\partial C/\partial z)/(C + k_d)^2$. These theoretical values are compared with the measured chemotactic speed to judge the virtue of these sensitivity models. Unfortunately, because the band formation is a continuous process, it is difficult to define when the band is formed. With this uncertainty and other experimental errors, the predictions of both KS and LS models are reasonable. From the formation of L-serine band experiment, we also confirmed the assumption of KS model that there is a threhold substrate concentration gradient.Below this gradient, bacteria will not be able to form a chemotactic band.

We have used a light scanning densitometry and moment analysis to study L-serine-limited band profiles. The chemotactic coefficient δ and the motility coefficient μ of bacteria in serine are estimated. The δ is $12.1 \times 10^{-6}\ cm^2/s$ and μ is $3.79 \times 10^{-6}\ cm^2/s$.

An improved theoretical model for bacterial self-correlation function based on two-state motions has been developed to obtain the mean square speed of run motion, V_2, and relative probability of twiddle vs. run at the centers of the chemotactic bands, $\beta = \tau_1/(\tau_1 + \tau_2)$. This modified model includes the effects of anisotropic bacterial motions in the direction of chemotaxis. Experimentally, a chopped

small angle light scattering technique has been developed to study the anisotropic bacteria motions in a L-serine-limited band. With this newly developed technique, the photon correlation functions in both perpendicular and parallel directions are measured simultaneously. This process ensures that the photon correlation functions are obtained from the same region of the chemotactic band. The microscopic parameters τ_1, τ_2, D_E and V_2 of bacterial motions using L-serine as attractant are extracted.

Finally, an attempt to connect the parameters in the macroscopic (δ,μ) and microscopic $(\tau_1, \tau_2, \langle V \rangle, \cos\theta)$ descriptions of chemotaxis has been made. The δ and μ derived from the microscopic parameters measured by the photon correlation functions are in qualitative agreement with those obtained from the study of macroscopic band profile. This demonstrates the validity of the linkage we have proposed between the macroscopic and microscopic parameters of bacterial chemotactic motions.

We are grateful to Anne Chen for assistance in taking data that allowed the construction of Fig. 2.

This work was supported by a National Science Foundation grant no. 8111534-0CM.

Received for publication 2 April 1985 and in final form 11 November 1985.

REFERENCES

1. Holz, M., and S. H. Chen, 1978. Quasi-elastic light scattering from migrating chemotactic bands of *Escherichia coli*. *Biophys. J.* 23:15–31.
2. Holz, M., and S. H. Chen, 1979. Spatio-Temporal structure of migrating chemotactic band of *Escherichia coli*. I. Traveling band profile. *Biophys. J.* 26:243–261.
3. Wang, P., and S. H. Chen. 1981. Quasi-elastic light scattering from migrating chemotactic bands of Escherichia coli, II. Analysis of anisotropic bacterial motions. *Biophys. J.* 36:203–219.
4. Beijerinck, M. 1893. Zenbl. Bakt. *Parasitkde.* 14:827.
5. Adler, J. 1966. Chemotaxis in bacteria. *Science* (*Wash. DC.*). 153:708–716.
6. Berg, H. C., and D. A. Brown, 1972. Chemotaxis in *Escherichia coli* analyzed by three-dimensional tracking. *Nature* (*Lond.*). 239:500–504.
7. Berg, H. C. 1975. Chemotaxis in bacteria. *Annu. Rev. Biophys. Bioeng.* 4:119–136.
8. Macnab, R. M. 1978. Bacterial motility and chemotaxis: the molecular biology of a behavioral system. *CRC Crit. Rev. Biochem.* 291–341.
9. Koshland, D. E., Jr. 1980. Bacterial Chemotaxis as a Model Behavioral System. Raven Press, New York.
10. Macnab, R. M., and D. P. Han. 1983. Asynchronous switching of flagellar motors on a single bacterial cell. *Cell.* 32:109–117.
11. Keller, G. F., and L. A. Segel. 1971. Traveling bands of chemotactic bacteria: a theoretical analysis. *J. Theor. Biol.* 30:235–248.
12. Mesibov, R., G. W. Ordal, and J. Adler. 1973. The range of attractant concentrations for bacterial chemotaxis and the threshold and size of response over this range—Weber law and related phenomena. *J. Gen. Physiol.* 62:203–223.
13. Lapidus, I. R., and R. Schiller. 1976. Model for the chemotactic response of a bacterial population. *Biophys. J.* 16(7):779–89.
14. Weibull, C. 1960. Movement. *In* The Bacteria, A Treatise on Structure and Function. I. C. Gunsalus and Y. Stainer, editors. Academic Press, Inc., NY. 1:153.
15. Scribner, T. L., L. S. Segel, and E. H. Rogers. 1974. A numerical study of the formation and propagation of traveling bands of chemotactic bacteria. *J. Theor. Biol.* 46:189.
16. Lapidus, I. R., and R. Schiller. 1974. A mathematical model for bacterial chemotaxis. *Biophys. J.* 14(11):825–34.
17. Bateman, H. 1954. Tables of integral transforms. Vol. 1, McGraw-Hill, Inc., New York.
18. Lapidus, I. R., and R. Schiller, 1978. A model for traveling bands of chemotactic bacteria. *Biophys. J.* 22(1):1–13.
19. Chen, S. H., and P. C. Wang. 1981. Light Scattering Measurement of the Two-State Motional Parameters of *Escherichia Coli* in Chemotactic Bands. *In* Biomedical Applications of Laser Light Scattering. D. Sattelle, et al., editor., North Holland.
20. Chen, S. H., W. B. Veldkamp, and C. C. Lai. 1975. Simple digital clipped correlator for photon correlation spectroscopy. *Rev. Sci. Instrum.* 46:1356.
21. Holz, M., and S. Chen, 1978. Tracking bacterial movements using a one-dimensional fringe system. *Opt. Lett.* 2:109.
22. S. Chandrasekhar. 1943. Stochastic problems in physics and astronomy. *Rev. Mod. Phys.* 15:1.
23. Oliver, J. C. 1974. Correlation techniques. *In* Photon Correlation and Light Beating Spectroscopy. H. Z. Cummins, and E. R. Pike, editors. Plenum Publishing Corp., New York.
24. Block, S. M., J. E. Segall, and H. C. Berg. 1982. Impulse responses in bacterial chemotaxis. *Cell.* 31:215–226.
25. Block, S. M., J. E. Segall, and H. C. Berg. 1983. Adaptation kinetics in bacterial chemotaxis. *J. Bacteriol.* 154:312–323.
26. Segel, L. A. 1977. A theoretical study of receptor mechanisms in bacterial chemotaxis *Soc. Ind. Appl. Math. J. Appl. Math.* 23:653.
27. Nossal, R. 1980. Mathematical theories of topotaxis biological growth and spread. *In* Mathematical Theories and Applications. W. Jager, H. Rost and P. Tautu, editors. Springer-Verlag, Heidelberg. 410.